DOI 10.1007/s11182-023-02954-9
Russian Physics Journal, Vol. 66, No. 4, August, 2023

MICROSTRUCTURE AND MECHANICAL PROPERTIES OF THE FERRITIC-MARTENSITIC STEEL EK-181 AFTER WARM ISOTHERMAL FORGING

V. V. Linnik,[1] N. A. Polekhina,[2] I. Yu. Litovchenko,[2] K. V. Spiridonova,[2] V. M. Chernov,[3] and M. V. Leontyeva-Smirnova[3]

UDC 669.018.25; 539.219; 539.25

The features of the microstructure and mechanical properties of the ferritic-martensitic steel EK-181 after warm isothermal forging in the ferritic region (tempforming) with the strain degree e ≈ 1.3 are studied. The formation of an inhomogeneous fragmented structure as a result of this processing is shown. The carbide subsystem does not change during processing. The mechanical properties of the steel have been studied under the conditions of tensile tests at 20 and 650°C accompanied by the microhardness measurements. It is shown that warm isothermal forging leads to some increase in the strength properties at room temperature. At an elevated temperature (650°C), the strength properties are comparable to those after traditional heat treatment (quenching and high-temperature tempering). The microhardness of steel after warm isothermal forging varied over the sample cross section from 2.7 GPa to 3.1 GPa. Tempering after multi-directional forging of the steel decreased its strength, but improved the plastic properties. The relationship between the microstructure and the mechanical properties of the EK-181 steel after isothermal forging in the ferritic region is discussed.

Keywords: ferritic-martensitic steels, warm multidirectional forging, grain refinement, substructure, mechanical properties.

INTRODUCTION

The 9–12% chromium ferritic-martensitic steels are structural materials promising for application in nuclear and thermonuclear reactors of new generation due to the achieved complex of physical and mechanical properties [1–4]. The steels of this class have good thermal conductivity, low thermal expansion coefficient, and low tendency to radiation swelling and radiation and helium embrittlement [5–9]. Exactly their operating temperatures and the degree of nuclear fuel burnup determine the efficiency of nuclear reactors. Higher operating temperatures and degrees of fuel burnout impose more stringent requirements to heat resistance of the structural materials. One of the methods for improving the high-temperature strength properties of the ferritic-martensitic steels is the use of thermomechanical treatments. The main idea of such treatments is the refinement of the grain/subgrain structure and the formation of an increased dislocation densities and fine particles [1–5].

The ferritic-martensitic steels with a chromium content of 9–12% have been studied in ample detail in the structural state after traditional heat treatment (THT) including normalization and high-temperature tempering [8, 10–

[1]National Research Tomsk State University, Tomsk, Russia, e-mail: lera.linnik.1999@mail.ru; [2]Institute of Strength Physics and Materials Science of the Siberian Branch of the Russian Academy of Sciences, Tomsk, Russia, nadejda89tsk@yandex.ru; litovchenko@ispms.ru; kseni_ya_almaeva@mail.ru; [3]Bochvar High-Technology Research Institute of Inorganic Materials, Moscow, Russia, e-mail: VMChernov@bochvar.ru; MVLeonteva-Smirnova@bochvar.ru. Original article submitted July 17, 2023.

TABLE 1. Elemental Composition of the EK-181 Steel (wt.%, Base Fe)

C	Cr	Mn	Mo	Nb	V	W	Ni	N	Si	Ce	Ti	B	Ta
0.16	11.17	0.74	0.01	0.01	0.25	1.13	0.03	0.04	0.33	0.15	0.05	0.006	0.08

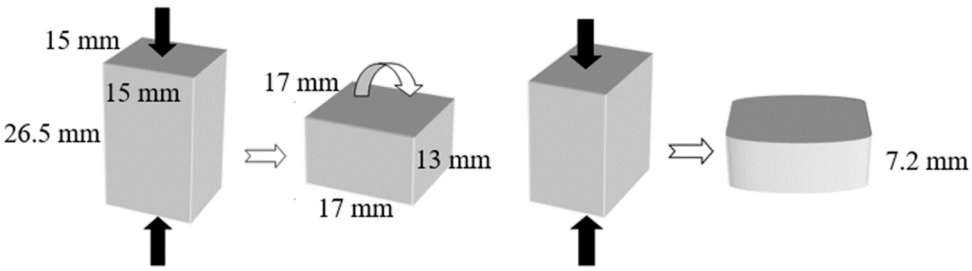

Fig. 1. Scheme of thermomechanical processing.

12]. In recent years, the influence of high-temperature thermomechanical treatment (HTMT) with plastic deformation in the austenitic region (ausforming) on the structural-phase states and strength properties of the ferritic-martensitic steels has been actively studied. In works [1–5, 10–12] it was shown that such treatments lead to a decrease in the average size of martensite blocks, an increase in the dislocation density, and contribute to an increase in the volume fraction of fine particles (under conditions of subsequent tempering). The microstructure changes provide an increase in the short-term high-temperature properties and creep resistance of these steels [1–5].

In works [13–15], thermomechanical treatments with plastic deformation were carried out by rolling of the low-carbon steels in the ferritic region at a temperature close to that of tempering. These treatments were termed tempforming (tempering forming). Tempforming is carried out at lower temperatures compared to ausforming, but is no less effective for modifying the steel microstructure [13, 14]. As a result of such processing, the average dimensions of structural elements are reduced. During rolling, grains/subgrains are formed that are flattened in the plane and elongated in the rolling direction [13–15]. In addition, tempforming promotes the release of finely dispersed carbide particles [13, 14]. These structural features increase the yield, tensile, and impact strengths compared to THT [13, 14]. The effect of tempforming on the microstructure and mechanical properties of the 12% chromium ferritic-martensitic steels has been little studied. The purpose of this work is to study the effect of plastic deformation in the ferritic region (tempforming) on the microstructure and mechanical properties of the promising low-activated Russian ferritic-martensitic steel EK-181. Multi-directional isothermal forging was chosen as a deformation method since it can be carried out under isothermal conditions of elevated temperatures (0.3–0.6 T_m) and makes it possible to realize higher degrees of plastic deformation compared to rolling [16, 17].

EXPERIMENTAL MATERIAL AND PROCEDURE

The elemental composition of the EK-181 ferritic-martensitic steel is presented in Table 1. Plastic deformation by isothermal forging was carried out in the structural state after traditional heat treatment (THT) of the steel that involved its normalization from $T = 1100$°C with exposure at the austenitization temperature for 1 h and tempering at $T = 720$°C for 3 h. The 26.5 × 15 × 15 mm^3 samples after THT were subjected to warm pressing with a single change of the deformation axis at a temperature of 720°C. The press tooling was at a temperature of 600°C. Between the passes, the sample was placed in an oven at a temperature of 720°C. The initial strain rate during pressing was 10^{-2} s^{-1}. During one upset, the workpiece was deformed by ~50%. The total accumulated strain was $e \approx 1.3$. After the deformation was completed, the samples were cooled in still air. The processing scheme is shown in Fig. 1. After isothermal forging, a part of the samples was annealed at $T = 720$°C for 1 h.

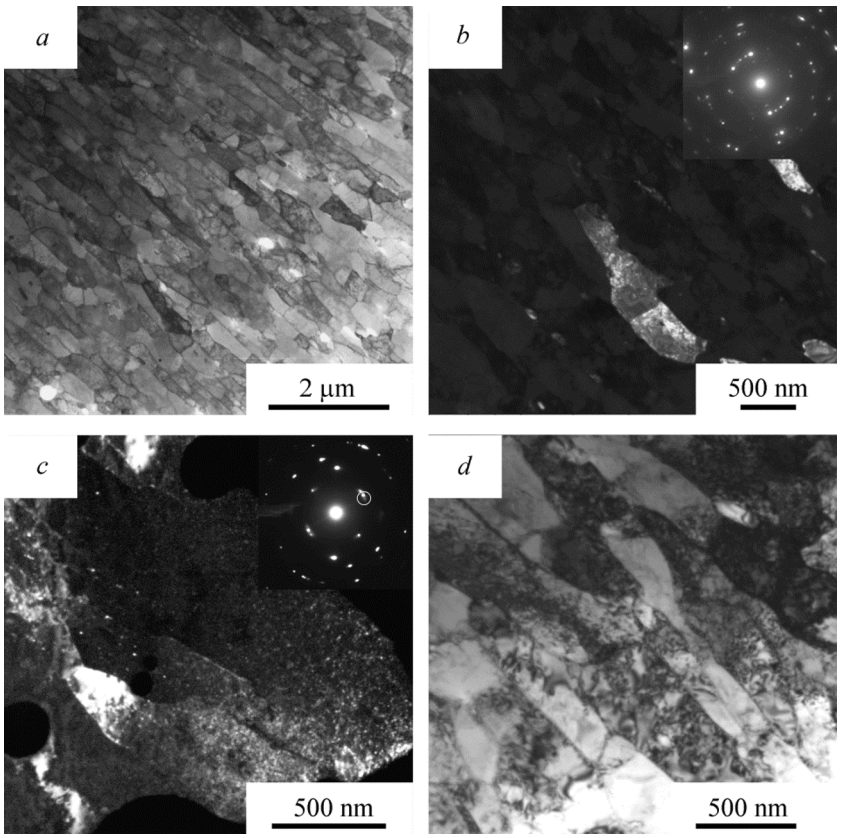

Fig. 2. TEM images of the EK-181 steel after thermomechanical treatment. Here *a* and *d* are the bright-field images and *b* and *c* are the dark-field images with selected area diffraction pattern. The combined reflections of matrix and MX particles are highlighted by the circle in Fig. 2*c*.

The steel microstructure was studied using a JEOL JEM-2100 transmission electron microscope (accelerating voltage 200 kV) equipped with an INCA Energy EDS X-ray microanalysis system (EDX). Thin foils were prepared by electropolishing in a chromic anhydride solution (50 g of CrO_3) of phosphoric acid (450 ml of H_3PO_4). The Vickers microhardness of the steel was measured using an AFFRI DM 8 microhardness tester with a load of 200 g for 10 s (20 prints on each sample). The mechanical tensile tests were carried out at a strain rate of $\approx 2 \cdot 10^{-3}$ s^{-1} at room temperature (20°C) on a MIM 2-50 testing machine and at a temperature of 650°C, close to the operating temperature of a nuclear reactor, on a high-temperature vacuum ($\approx 7 \cdot 10^{-3}$ Pa) testing machine PV-3012M using the samples with a gaging section length of 13 mm and a cross section of 2×1 mm^2.

RESULTS AND DISCUSSION

Figure 2 shows the steel microstructure images obtained by transmission electron microscopy (TEM). An examination of thin foils showed that after the thermomechanical treatment, the microstructure of the steel EK-181 consisted of fragmented martensitic laths. The dark-field image (Fig. 2*b*) shows that the martensitic laths are broken into fragments with low-angle misorientation boundaries along their lengths. The average length of such fragments is 850 nm, and their width is 280 nm. In the combined reflection of the matrix and the MX phase (M = V, X = C, N) of the dark-field image, there are fine particles 5–10 nm in size. In the martensitic structure, a high density of dislocations is locally observed (Fig. 2*c*) reaching values of $(5–9) \cdot 10^{11}$ cm^{-2}, which is several times higher than after THT [10]. Also

TABLE 2. Elemental Composition of the Dispersed Particles and Matrix of the Ferritic-Martensitic Steel EK-181 after TMT (at Points 1–5 in Fig. 3*a*)

Point number	Ti	V	Cr	Mn	Fe	Zr	Ta	W
1	0.45	2.85	1.13	0	0.27	0	95.12	2.87
2	0.32	0.51	52.38	1.28	26.37	0	0.22	16.85
3	0.14	1.07	53.98	0.92	29.07	0.57	0.28	9.47
4	0.22	1.67	57.93	1.02	26.25	0.51	0	7.67
5	0.02	0.11	10.95	1.05	84.59	0.50	0.86	1.92

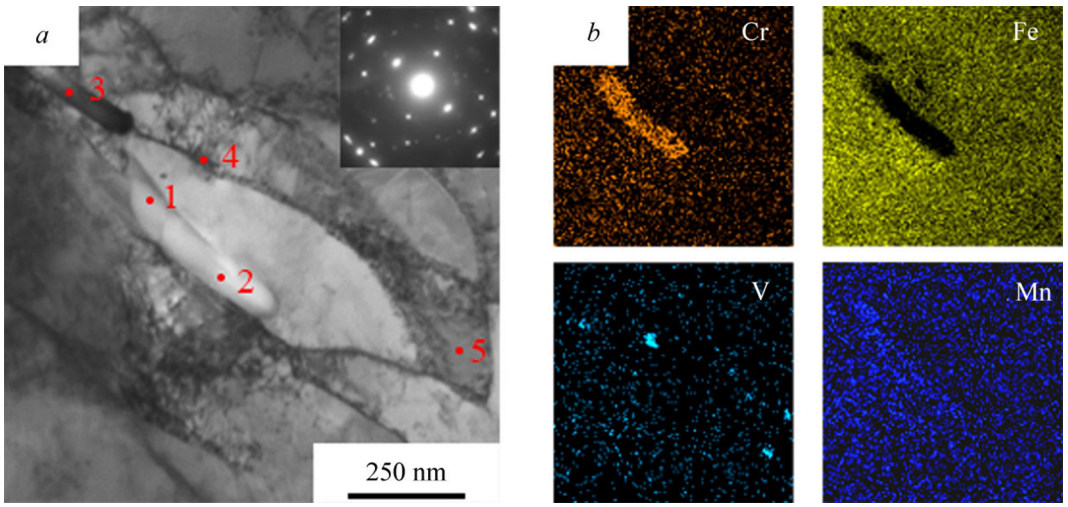

Fig. 3. TEM images of the $M_{23}C_6$ and MX particles after TMT including the bright-field image with selected area diffraction pattern (*a*) and the local elemental maps of EDX microanalysis (*b*).

locally observed are the areas represented by the tempered martensite and ferrite grains with dislocation density of ~10^{10} cm^{-2}, which is an order of magnitude lower.

The TEM images (Fig. 3) exhibit coarse particles along the boundaries of martensite lamellae. Our EDS X-ray microanalysis (Fig. 3 and Table 2) and TEM analysis of the diffraction patterns showed that these particles are carbides of the $M_{23}C_6$ type (M = Fe, Cr) and carbonitrides of the MX type based on vanadium. The average dimensions of the $M_{23}C_6$ carbides after warm isothermal forging were from 85 to 130 nm, that is, slightly smaller than in the case of traditional heat treatment.

The volume fractions of the second-phase particles (V(CN) and $M_{23}C_6$) after the thermomechanical treatment are comparable to those after THT. This may be due to the fact that plastic deformation at elevated temperatures was carried out for a limited time insufficient for the volume fractions of dispersed particles to change.

Our study of the mechanical properties showed that the thermomechanical processing by isothermal forging led to an increase in the tensile and yield strengths at room temperature compared to the state after THT. The tensile strength after TMT reached 917 MPa, which is 7% higher than that of the traditionally heat-treated sample (860 MPa). Note that the plasticity practically did not change (12.2% after TMT and 13% after THT). An additional annealing at 720°C for 1 h to relieve the internal stresses after deformation led to a noticeable decrease in the ultimate strength down to 732 MPa and an increase in the elongation to failure up to 16.3%. At the elevated test temperature (650°C), no significant change was observed in the strength properties after TMT by isothermal forging compared to THT. The yield and ultimate strengths of the sample after TMT were 296 MPa and 330 MPa, respectively, whereas after THT,

they were 309 MPa and 327 MPa. At the same time, a slight increase in plasticity was also observed, which was 17% after TMT and 13% after THT. Annealing after TMT led to a decrease in the yield and tensile strengths at the elevated test temperatures down to 245 MPa and 297 MPa, respectively, and to an increase in ductility up to 28%.

After traditional heat treatment, the microhardness values were homogeneous over the sample and, on average, were found to be equal to 2.81 GPa. After deformation by pressing, the microhardness values changed from 2.7 GPa in the center of the sample to 3.1 GPa along the edges of the deformed workpiece. The average values of the microhardness of the sample in the state after deformation by pressing were equal to 2.91 GPa.

Thus, the above-described thermomechanical treatment led to a noticeable refinement of the microstructure compared to the state after traditional heat treatment. We have found out that warm plastic deformation under the conditions of isothermal forging promotes the formation of new subboundaries, thereby halving the width of the martensitic lamellae and decreasing their length by a factor of 3.5 compared to THT. The refinement of the subgrain structure and the increase in the dislocation density contributed to some increase in the steel strength properties. The microstructure formed in the sample as a result of TMT by isothermal forging was inhomogeneous. Therefore, the microhardness near the center of the sample and on the periphery differed markedly. It is likely that insignificant effects of strengthening under the conditions of deformation by isothermal forging are due to the fact that the test pieces included both the central and peripheral parts of the sample with different degrees of deformation, in which the dislocation density might differ by an order of magnitude. In works [15, 17, 18], it has been shown that the degree and temperature of deformation and the number of passes have a significant effect on the dimensions of microstructure elements and their homogeneity over the sample volume. To form a more homogeneous microstructure under the conditions of the studied thermomechanical treatment, a higher degree of deformation and a larger number of upsets are required.

CONCLUSIONS

The effect of thermomechanical treatment on the microstructure and mechanical properties of a low-activation 12% chromium ferritic-martensitic steel EK-181 has been studied, including warm isothermal forging in the region of the α-phase persistence (tempforming). It was shown that after TMT, the steel microstructure was represented by the fragmented martensitic laths with the coarse chromium-based $M_{23}C_6$ carbides and vanadium-based MX type carbonitrides as well as by finely dispersed (5–10 nm) particles of the same phase. A decrease in the average length and width of the martensitic laths compared to the traditional treatment was found. The dislocation density after isothermal forging locally increased to $(5–9)\cdot10^{11}$ cm^{-2}; however, there were regions in which this value was smaller by an order of magnitude. The sizes of coarse $M_{23}C_6$ particles were slightly smaller compared to those after THT. The volume fractions of dispersed particles were comparable to the corresponding values after THT. The features of the microstructure formed as a result of the warm isothermal forging led to some increase in the tensile and yield strengths of the steel at room temperature. The microhardness in the center and on the periphery of the samples was 3.1 GPa and 2.7 GPa, respectively. At the same time, its average values were higher compared to those after THT. A high-temperature annealing after TMT led to a decrease in the yield and ultimate strengths compared to THT and caused an increase in plasticity.

This work was performed according to the Government Research Assignment for the Institute of Strength Physics and Materials Science of the Siberian Branch of the Russian Academy of Sciences (the ISPMS SB RAS) (Project No. FWRW-2021-0008). The research was carried out with the equipment of the Share Use Centre “Nanotech” of the ISPMS SB RAS.

REFERENCES

1. X. Jin, Sh. Chen, and L. Rong, Mater. Sci. Eng. A, **712**, 97 (2018); https://doi.org/10.1016/J.MSEA.2017.11.095.
2. L. Tan, J. T. Busby, P. J. Maziasz, and Y. Yamamoto, J. Nucl. Mater., **441**, 713 (2013); https://doi.org/10.1016/j.jnucmat.2012.10.015.
3. Sh. Li, Z. Eliniyaz, F. Sun., *et al*., Mater. Sci. Eng. A, **559**, 882 (2013); https://doi.org/10.1016/j.msea.2012.09.040.
4. Z. Xu, Y. Shen, Z. Shang, *et al*., J. Nucl. Mater., **509**, 355 (2018); https://doi.org/10.1016/j.jnucmat.2018.04.025.
5. J. H. Zhou, Y. F. Shen, Y. Y. Hong, *et al*., Mater. Sci. Eng. A, **769**, 138471 (2020); https://doi.org/10.1016/j.msea.2019.138471.
6. Sh. Yin, Y. Liu, and F. Zhao, Fusion Eng. Des., **173**, 112785 (2021); https://doi.org/10.1016/j.fusengdes.2021.112785.
7. P. Shruti, T. Sakthivel, G. V. S. Rao, *et al.*, Metall. Mater. Trans. A., **50**, No. 10, 4582 (2019); https://doi.org/10.1007/s11661-019-05364-0.
8. P. Prakash, J. Vanaja, N. Srinivasan, *et al.*, Mater. Sci. Eng. A, **724**, 171 (2018); http://dx.doi.org/10.1016/j.msea.2018.03.080.
9. A. Puype, L. Malerba, N. De Wispelaere, *et al.*, J. Nucl. Mater., **494**, 1 (2017); http://dx.doi.org/10.1016/j.jnucmat.2017.07.001.
10. N. A. Polekhina, V. V. Linnik, I. Yu. Litovchenko, *et al*., Metals, **12**, 1928 (2022); https://doi.org/10.3390/met12111928.
11. I. Litovchenko, K. Almaeva, N. Polekhina, *et al*., Metals, **12**, No. 1, 79 (2022); https://doi.org/10.3390/met12010079.
12. K. V. Almaeva, N. A. Polekhina, V. V. Linnik, and I. Yu. Litovchenko, AIP Conf. Proc., **2167**, 020013 (2019); https://doi.org/10.1063/1.5131880.
13. A. Dolzhenko, A. Pydrin, S. Gaidar, *et al*., Metals, **12**, 48 (2021); https://doi.org/10.3390/met12010048.
14. A. Dolzhenko, R. Kaibyshev, and A. Belyakov, Metals, **10**, 1566 (2020); https://doi.org/10.3390/met10121566.
15. Y. Kimura and T. Inoue, ISIJ Int., **60**, 1108 (2020); https://doi.org/10.2355/isijinternational.ISIJINT-2019-726.
16. H. Jiang, Y. Liu, Y. Wu, *et al*., J. Mater. Eng. Perform., **28**, 3505 (2019); http://dx.doi.org/10.1007/s11665-019-04111-1.
17. Y. Nakao and H. Miura, Mater. Sci. Eng. A, **528**, 1310 (2011); http://dx.doi.org/10.1016/j.msea.2010.10.018.
18. V. Soleymani and B. Eghbali, J. Iron Steel Res. Int., **19**, 74 (2012); http://dx.doi.org/10.1016/S1006-706X(12)60155-1.